Plugging mechanism of open-ended piles

Mécanisme d'obturation des pieux à extrémité ouverte

Y. Kikuchi & Y. Morikawa
Port & Airport Research Institute, Yokosuka, Japan
T. Sato
Toa Corporation, Yokohama, Japan

ABSTRACT
For the past 50 years, the pile foundations of port facilities in Japan have been constructed by means of driving steel pipe piles. Although the pile diameter and length have been modified over the years, the design method has hardly changed, and it has always been difficult to evaluate the bearing capacity at the pile base. This paper introduces the changes adopted for pile foundations used in Japan's port facilities and presents the latest studies on the bearing capacity at the base of open-ended piles. Important facts on the plugging phenomena of open-ended piles are presented and the plugging mechanism of open-ended piles is discussed.

RÉSUMÉ
Pendant ces 50 dernières années, les fondations sur pieux des installations portuaires au Japon ont été construites avec des pieux tubulaires en acier battus. Bien que le diamètre et la longueur du pieu aient été modifiés au cours des années, la méthode de conception n'a guère subi de changements. En outre, l'évaluation de la capacité portante à la base des pieux a toujours posé des problèmes jusqu'ici. Cet article présente les changements adoptés pour les fondations sur pieux, utilisées dans les installations portuaires du Japon, et expose les dernières études sur la capacité portante à la base des pieux à extrémité ouverte. Ces études ont présenté des faits importants sur les phénomènes d'obturation des pieux à extrémité ouverte et ont discuté le mécanisme d'obturation des pieux à extrémité ouverte.

Keywords : steel pipepiles, base bearing capacity, field loading test, laboratory test, PIV

1 INTRODUCTION

For the past 50 years, the pile foundations of port facilities in Japan have been constructed by means of driving steel pipe piles.

Two investigations on the design situations of piles were conducted. One of them was conducted in 1967 and the other was conducted in 2003(Kikuchi, 2008). These results show that piles with a diameter of about 1300 mm have been used in recent years, whereas piles with a diameter of 800 mm or less were used in the 1960s. The change in the distribution of the embedded length of piles between the two investigations shows that the embedded length of some piles has exceeded 60 m in recent years, whereas it was about 30 m in the 1960s.

These changes have been driven by the need for piles with large bearing capacity to support the increased loads of larger super-structures and improvements in construction technology and equipment. However, the changed pile diameter and embedded length requires a change in the equation used to estimate the static bearing capacity for the design, the design method has hardly changed and it has created considerable uncertainty about the base bearing capacity.

This paper experimentally studied the mechanism of the plugging of open-ended piles to improve the accuracy of estimating the toe bearing capacity of piles.

2 PREVIOUS STUDIES

The base bearing resistance R_b of open-ended piles is the sum of the toe resistance R_{toe} of the annular pile base and the inner shaft friction resistance R_{fi}. The ratio of the base resistance of the open-ended pile against the resistance of the closed-ended pile R_{PC} is defined by the plugging efficiency $\eta = (R_{toe}+R_{fi})/R_{PC}$ (AIJ, 2001). Yamagata et al. (1973) proposed a practical method of estimating the bearing capacity of toe resistance Q_{toe} with SPT-N values. De Nicola et al. (1997) proposed it with CPT resistance. Regarding the inner friction capacity Q_{fi}, many theoretical (e.g. Yamahara, 1969) and experimental (Matsumoto et al., 2007) studies were conducted. These studies revealed that increasing the inner surface area such as by using separation walls effectively increases the bearing capacity of open-ended piles. Sufficient penetration to the bearing layer is also known to increase the inner friction of open-ended piles.

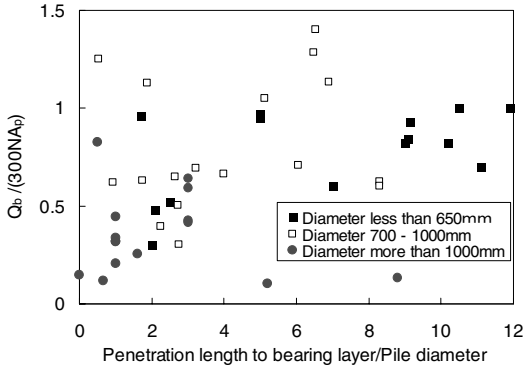

Figure 1. Relationship between penetration ratio (L/D) and apparent plugging ratio.

Figure 1 shows the relationship between the penetration ratio to the bearing layer and the apparent plugging ratio of field loading test results. This apparent plugging ratio was obtained by dividing the measured base resistance by the base bearing capacity of closed-ended piles calculated from the equation proposed in JTSP (OCDI, 2002). The data plotted in the figure are from the JASPP manual (2004) and original data. The weak relationship means that an increase in the penetration ratio is not

Proceedings of the 17th International Conference on Soil Mechanics and Geotechnical Engineering
M. Hamza et al. (Eds.)

doi:10.3233/978-1-60750-031-5-1370

a governing factor for the increase of bearing capacity or for constructing the plug.

Figure 2 shows the relationship between pile diameter and apparent plugging ratio for the same data shown in Fig. 1. This figure shows that the pile diameter is an important factor for the plugging, even though there is large variance in the relationship.

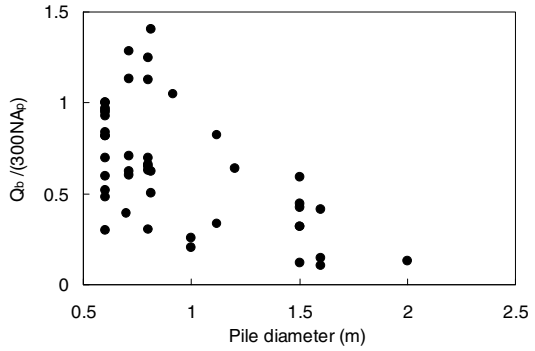

Figure 2. Relationship between pile diameter and apparent plugging ratio.

Otani et al. (2003) discussed the deformation characteristics of the ground surrounding the pile base based on X-ray CT scanner images. Model piles with several kinds of toe shape were inserted into the model ground vertically and the failure patterns were examined with an investigation of the change in density of the ground by X-ray CT images. However, the problems of continuous deformation characteristics of the ground during the pile penetration and soil that penetrated the open-ended piles were not adequately discussed.

3 BASE BEARING CAPACITY OF OPEN-ENDED PILES

To estimate the bearing capacity of bridge foundations, a series of field axial loading tests of piles was conducted in Tokyo Bay (Kikuchi et al., 2007).

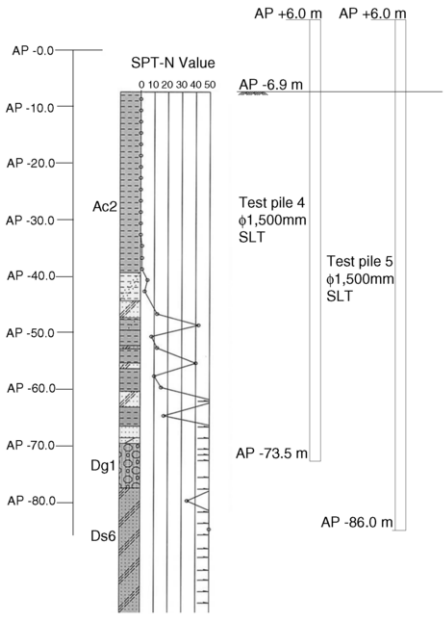

Figure 3. Overview of soil boring log and embedment of test piles.

Figure 3 shows the ground conditions where the tests were conducted and the embedded depth of test piles. It can be seen from the figure that a diluvial sandy gravel layer appears around AP-69 m and following a few weak layers in the sandy gravel layer around AP-80 m, a solid sandy layer appears around AP-82 m. Steel pipe piles of 1500 mm in diameter and 28 mm in radial thickness were hammer-driven into the sandy gravel layer and sandy layer, in order to obtain the characteristics of bearing capacity under two conditions. In these load tests, the axial force acting on a pile was measured by attaching strain gauges to the pile, and concurrently, the settlements of the pile both at the toe and the head were measured using settlement gauges.

Figure 4 shows an enlarged view of the axial force distribution around the pile base when the pile was loaded at around the maximum load in the test. Open circles show measured axial force. From the figure, axial force dramatically decreased at the depth of –72.75m. This kind of axial force reduction was not observed at the lower level of loading but was observed as the load was increased. Focusing on this phenomenon, ground solidity did not change at around this depth. Judging from the test results for Pile No. 5 which was embedded more deeply, it was unlikely that peripheral friction became large at this point (see Fig. 5). It can be concluded that a sharp change in axial force might have been caused by skin friction on the inner side of the pile as shown in Fig. 5. As shown in Fig. 4, the total bearing capacity at the pile base could be obtained by extrapolating the measured values of axial force within the assumed bearing layer to the level of the lower pile end (Point B).

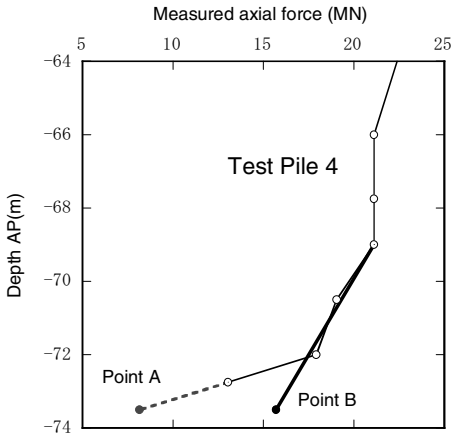

Figure 4. Axial force distribution at the base of Pile No. 4.

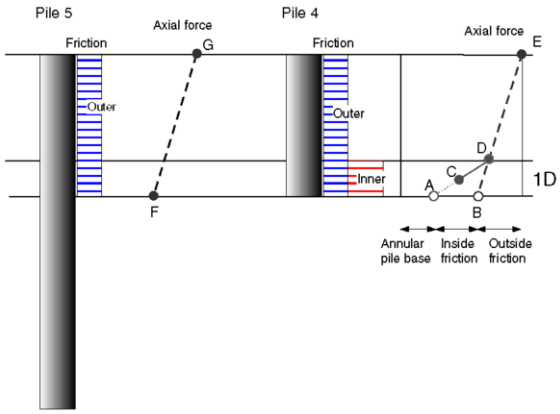

Figure 5. Relationship between axial force distribution and friction.

Assuming that the load at Point A obtained by extrapolating the measured value is the resistance of the annular pile base, the difference between the load at Point B and the load at Point A could be regarded as the plug resistance due to inner friction. Figure 6 shows the relationship between total base resistance, inner friction resistance, and resistance of the annular pile base. In the figure, at the secondary critical resistance which was defined as the resistance at the toe settlement of 10% of the pile

diameter, the total base resistance shows an increase. The resistance of the annular pile base reached almost the maximum value when the settlement of the pile base was about 50 mm, while the inner friction resistance was still increasing when settlement was more than 150 mm. In this way, the resistance of the annular part of the pile increases at small settlement, while the resistance of the inner friction increases with large settlement.

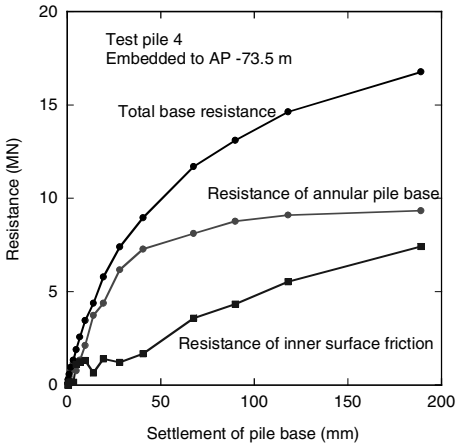

Figure 6. Resistance at base of Pile No. 4.

4 PENETRATION EXPERIMENT OF OPEN-ENDED PILES IN MODEL GROUND

To examine the plugging effect, two series of penetration experiments were performed on open-ended piles in a model ground. In the first series, the bearing capacity of open- and closed-ended piles was observed. In the second series, the deformation situation of the ground near the pile base during pile penetration was observed using a micro-focus X-ray CT scanner.

4.1 *Large-scale pile penetration test in model ground*

The sand used for the model ground was Souma sand #4 having a soil particle density equal to 2.644 g/cm^3, minimum and maximum void ratios of 0.634 and 0.970, respectively and D_{50} = 0.7 mm. Dried Souma sand was packed to a thickness of 2.8 m in a container of 6 m in length, 3 m in width, and 3 m in depth. The relative density of the model ground was about 40%.

After preparing the model ground, a model pile was driven into the ground. This pile was 20 cm in outer diameter, 17 cm in inner diameter, 2 m in length, and was made of acrylic resin. The pile could be used as either a closed-end or open-ended pile by attaching or removing a bottom plate (Mizutani et al., 2003).

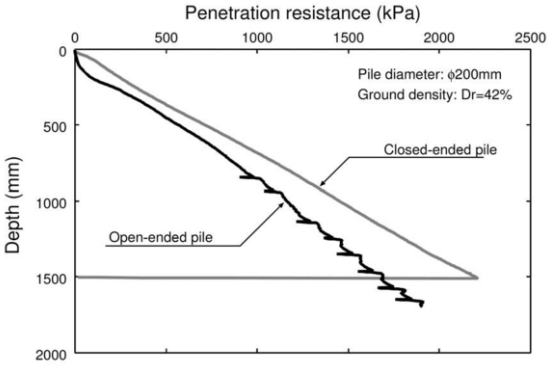

Figure 7. Relationship between depth and penetration resistance.

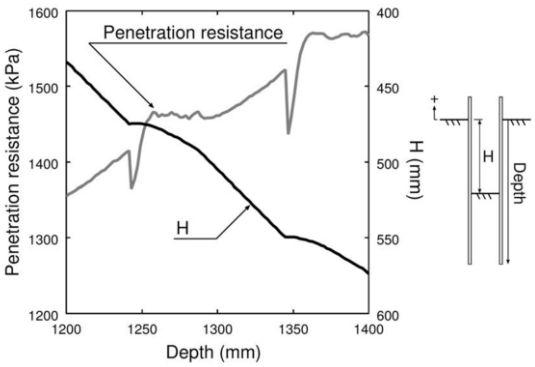

Figure 8. Cyclic change of penetration resistance of open-ended pile compared with the height change of inside ground.

The pile was driven into the model ground statically at a rate of 20 mm a minute. Penetration resistance at the pile head and height change of the surface of the ground inside open-ended piles were measured continuously during penetration.

Figure 7 shows the relationship between the depth and the penetration resistance of the model piles. In these experiments, more than 90% of the penetration resistance was base resistance. After the penetration depth reached 800 mm, a remarkable change occurred in the penetration resistance of the open-ended pile: the penetration resistance increased and decreased periodically.

An enlarged cycle of this periodical change in penetration resistance is depicted in Fig. 8, compared with the height change of the inside ground surface of the open-ended pile. The cyclic behavior included four phases: 1) A sudden reduction in penetration resistance took place at about 1250 mm in depth. At that moment, the height change of the inside ground surface, which is denoted by 'H' in Fig. 8, came to a standstill. 2) The penetration resistance increased rapidly, while the height of the inside ground surface stood at about 475 mm. 3) From the penetration depth of 1260 to 1300 mm, the penetration resistance stopped increasing and remained at a constant value. In the meantime, H increased gradually; however, the increment of H was less than the increment of the pile penetration depth. 4) After the depth exceeded 1300 mm, the penetration resistance started to increase again. At this stage, the increment of H was equal to the increment of the penetration depth, that is, the inside soil and the open-ended pile itself penetrated into the model ground as one body.

Thus, the open-ended pile could not continuously remain in the fully-plugged condition, and intermittent plugging was observed. This sort of phenomenon has already been reported by Hight et al. (1996) who also conducted other types of model tests.

4.2 *Observation of deformation of surrounding ground during penetration of open-ended pile*

A plug in the pile tip part occurs under the effect of the interaction between the pile and the ground. Therefore, it is necessary to know the deformation situation of the ground near the pile tip. The inner ground was therefore observed using a micro-focus X-ray CT scanner.

The CT scanner used in this research was the micro-focus type, with maximum voltage and output of 225 kV and 135 W, respectively. Multiple cross-sectional images were taken by using the 3D cone-beam imaging function, enabling detailed observation of the deformation occurring in the ground.

Dry Toyoura sand (D_{50} = 0.2 mm, U_c = 1.6) with relative density of 65% was packed in an acrylic container (100 mm in inner diameter), and the ground height was adjusted to 270 mm. An overburden pressure of 2.5 kPa was applied using stainless

steel balls (2 mm in diameter). In order to investigate the movement of the ground from the X-ray CT scanning results, a layer of iron particles of 0.3 mm in diameter was used. Closed-ended and open-ended aluminum piles (outer diameter: 15 mm, length: 140 mm) were used in the experiment. The thickness of the open-ended pile was 1 mm. The piles were driven into the ground at a rate of 1 mm/min and the maximum penetration depth was 81 mm. The entire pile penetration experiment was conducted in the micro-focus X-ray CT scanner room. To obtain CT images during the experiment, pile penetration was stopped at intervals of 3 mm and X-ray CT scanning was performed (Kikuchi et al., 2008).

Figure 9 shows the movement of the particles with points and lines as extracted from the CT images. The points are the positions of the particles relative to the pile at each 3-mm step of penetration, and the lines are the particle routes. With the closed-ended pile, the particles below the pile showed a tendency to be pushed out to the outside of the pile tip. A clear wedge was produced at the bottom of the pile base. Some of the particles below the pile were caught at the surface of the wedge, and some were discharged to the side of the pile at the edge and then moved along the pile. On the other hand, in the case of the open-ended pile, the movement of particles below the pile differed in that the particles were able to move upward and penetrate into the pile.

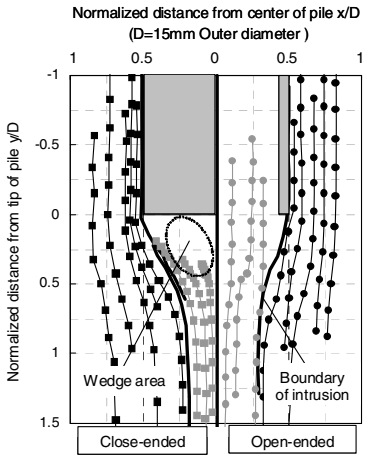

Figure 9. Movement of particles.

In order to examine in further detail the ground behavior, the PIV (Particle Image Velocimetry) method was applied to the CT images taken and the results were used for deformation analysis of the model ground. In this experiment, Souma sand #4 (D_{50} =0.7 mm, U_c = 1.6, Dr = 65%) and aluminum pile with 32 mm in outer diameter and 1.5 mm in annular thickness were used to observe the ground behavior by PIV. The model pile was set up in the model ground at the initial embedment depth of 50 mm. Maximum penetration depth was 51 mm from the embedded depth. Other testing conditions were the same as those used in previous experiments.

The vectors of ground displacement that were measured by the PIV method are shown in Fig. 10. The displacement vectors were measured on two-step CT images at each 3 mm of penetration. As it is difficult to recognize the deformation of the ground in this figure in detail, major displacements are indicated by arrows in the figure. The inner soil of the pile at the initial stage created a plug. While the penetration depth increased slightly, this plug was almost broken by the increased resistance below the pile base. From 3 to 33 mm of penetration, the transient process of the plugging effect occurred and small displacement was observed in the ground inner and below the pile. The plug appeared again after the penetration of 36 mm. During reconstruction of the plug, the plug was constructed from the inner pile surface to the central part of the pile radius.

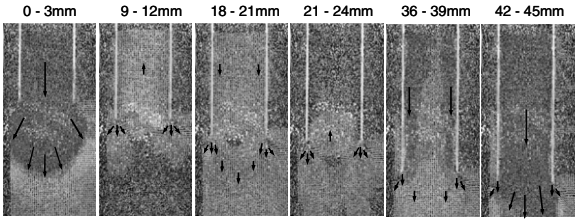

Figure 10. Image of the ground displacement from CT images using PIV method. Arrows show the major direction and amount of displacement of the ground during the 3 mm penetration. The penetration depth is presented above each picture.

5 CONCLUSIONS

This study examined the plugging mechanism of open-ended piles with field loading tests on real piles, laboratory experiments on model open-ended piles, and small-scale pile penetration experiments for observing ground deformation. The following conclusions were obtained:

(1) The resistance of the annular pile body reached almost the maximum value at a small settlement of the pile end (about 3% of the pile diameter), while the inner friction resistance required further settlement to reach the maximum value.
(2) The plugging phenomenon at the pipe pile base depends on the balance between the ground reaction and frictional resistance inside the pile and the weight of the soil.
(3) An open-ended pile could not continuously maintain the fully-plugged condition, and intermittent plugging was observed.

REFERENCES

Architectural Institute of Japan. 2001. Recommendations for the Design of Building Foundations, p. 207, (in Japanese).

De Nicola, A. and Randolph, M.F. 1997. Plugging behaviour of driven and jacked piles in sand, Geotechnique Vol.47, No.4, pp. 841-856.

Hight, D., Lawrence D., Farquhar, G., Milligan, G., Gue, S., and Potts, D. 1996. Evidence for scale effects in the end bearing capacity of open-ended piles in sand, Proc. of 28th OTC, pp.181-192.

Japanese Association for Steel Pipe Piles. 2004. Steel pipe pile – its design and construction, p. 110 (in Japanese).

Kikuchi, Y. 2008. Bearing capacity evaluation of long, large-diameter, open-ended piles, Proc. of 6th Int. Conf. on Case histories in Geotechnical engineering, SAOP1.

Kikuchi, Y., Mizutani, M. and Yamashita, H. 2007. Vertical bearing capacity of large diameter steel pipe piles, Advances in Deep Foundations, Proc. of IWDPF07, pp.177-182.

Kikuchi, Y., Morikawa, Y., and Sato, T. 2008. Plugging mechanism in a vertically loaded open-ended pile Proc. of 2nd BGA Int. Conf. on Foundations, pp.169-180.

Matsumoto, T., Kittiyodom, P., and Shintani, T. 2007. Trend of research and practice of pile foundations in Japan, Advances in Deep Foundations, Proc. of IWDPF07, pp.143-173.

Mizutani T, Kikuchi Y and Taguchi H. 2003. Cone penetration tests for the examination of plugging effect of open-ended piles, Proc. of BGA Int. Conf. on Foundations, pp.655-664.

Overseas Coastal Area Development Institute of Japan. 2002. Technical standards and commentaries for port and harbour facilities in Japan. pp. 286-287.

Otani J, Hironaka J and Mukunoki T. 2003. Visualization of failure patterns under vertically loaded pile foundation using X-ray CT method, Proceedings of 12th Asian Regional Conference on Soil Mechanics and Geotechnical Engineering, Singapore, Vol. 1, pp 973-976.

Yamagata, K. and Nagai, K. 1973. Consideration of an open-ended steel pipe pile (No. 2), Journal of Architecture and Building Engineering, No. 213, (in Japanese).

Yamahara, H. 1969. Bearing mechanism of steel pipe pile and its application, Tsuchi-to-Kiso, Vol. 17. No. 11, pp.19-27, (in Japanese).